30
3/31/87 JGM

3 Dist   5-29930

DR 0200-3

SLAC-PUB--4246

DE87 007348

SLAC – PUB – 4246
February 1987
(N)

Study of the Radiative Decay $J/\psi \to \gamma\eta\pi^+\pi^-$ †

J.J. Becker, G.T. Blaylock, T. Bolton, J.S. Brown, K.O. Bunnell, T.H. Burnett, R.E. Cassell, D. Coffman, V. Cook, D.H. Coward, H. Cui, S. Dado, D.E. Dorfan, G. Dubois, A.L. Duncan, G. Eigen, K.F. Einsweiler, D. Favart, B.I. Eisenstein, T. Freese, G. Gladding, F. Grancagnolo, A. Guy, R.P. Hamilton, J. Hauser, C.A. Heusch, D.G. Hitlin, L. Köpke, W. S. Lockman, U. Mallik, C. G. Matthews, P.M. Mockett, R.F. Mozley, B. Nemati, A. Odian, J. Parker, R. Partridge, J. Perrier, S.A. Plaetzer, J.D. Richman, J.J. Russell, H.F.-W. Sadrozinski, M. Scarlatella, T.L. Schalk, R.H. Schindler, A.Seiden, C. Simopoulos, A.L. Spadafora, I. Stockdale, W. St khousen, J.J. Thaler, W. Toki, B. Tripsas, Y. Unno, F. Villa, S. Wasserbaech, A. Wattenberg J.Weinstein, N. Wermes, H.J. Willutzki, D. Wisinski, W.J. Wisniewski, G. Wolf, R. u, Y. Zhu

The MARK III Collaboration

California Institute of Technology, Pasadena, CA 91125
University of California at Santa Cruz, Santa Cruz, CA 95064
University of Illinois at Urbana-Champaign, Urbana, IL 61801
Stanford Linear Accelerator Center, Stanford, CA 943
University of Washington, Seattle, WA 98195

Abstract

The Mark III collaboration has performed a high statistics study of the reaction $J/\psi \to \gamma\eta\pi^+\pi^-$, with two different final states of the η, $\eta \to \gamma\gamma$ and $\eta \to \pi^0\pi^+\pi^-$. Both modes have a broad structure from 1.2 to 1.9 GeV/c^2 and two structures, which decay via $\delta^\pm\pi^\mp$, $\delta^\pm \to \eta\pi^\pm$, are identified at 1.28 and 1.39 GeV/c^2. No signal is observed in the $\iota(1440)$ signal region.

Contributed to the 23rd International Conference on High Energy Physics, Berkeley, CA., July 16-23, 1986

† This work supported in part by the Department of Energy, under contracts DE-AC03-76SF00515, DE-AC02-76ER01195, DE-AC03-81ER40050, DE-AM03-76SF0034, and by the National Science Foundation.

1. Introduction

This paper presents preliminary results on the radiative decay, $J/\psi \to \gamma\eta\pi^+\pi^-$. Established resonances accessible in the $\eta\pi\pi$ channel are the η', the $\iota(1440)$, the $E(1420)$, the $D(1285)$ and the pseudoscalar $\eta(1275)$. The Crystal Ball collaboration has previously reported a broad enhancement in this channel which could contain these states.[1]

The $\iota(1440)$ has the largest single radiative J/ψ branching ratio other than the η_c and has been observed only in the $K\bar{K}\pi$ mode.[2] Some partial wave analyses suggested that the $\iota(1440)$ and the $E(1420)$, which may be the same state, both have large quasi-two body decays to $\delta\pi$, $\delta \to K\bar{K}$.[3] Since the δ has a well established decay to $\eta\pi$ there should be a large decay rate of $\iota(1440)$ into $\eta\pi\pi$ and consequently it should be observed in the J/ψ radiative decay to $\eta\pi\pi$.[4] Evidence for the decay, $E(1420) \to \delta\pi, \delta \to \eta\pi$, has been presented in several experiments and hence if the $E(1420)$ is produced in radiative J/ψ decays it could be seen in the J/ψ radiative decay to $\eta\pi\pi$.[5]

The axial vector $D(1285)$ is often produced in hadronic production along with the $E(1420)$ and it decays to $\delta\pi$.[6] Radiative J/ψ decays to the axial vector states have not been seen and an upper limit has been published for the $D(1285)$.[7] The $\eta(1275)$ is the radially excited η candidate that decays to $\eta\pi\pi$ and has been seen only in partial wave analyses.[8] The $\eta(1275)$ may be expected because the radiative J/ψ branching ratios to the η and the η' are very large.

The reaction $J/\psi \to \gamma\eta\pi^+\pi^-$ is studied in two final states with the $\eta \to \gamma\gamma$ and $\eta \to \pi^0\pi^+\pi^-$. This paper is organized into; 1) a brief description of the apparatus, 2) the analysis of the modes $J/\psi \to \gamma\eta\pi^+\pi^-$, $\eta \to \gamma\gamma$ and $J/\psi \to \gamma\eta\pi^+\pi^-$, $\eta \to \pi^0\pi^+\pi^-$ and 3) a discussion of the results.

2. Mark III Detector

The Mark III apparatus is a general purpose magnetic solenoidal detector optimized for SPEAR energies. A detailed account has been given elsewhere.[9] The relevant detectors for this analysis are the drift chamber and the electromagnetic calorimeter. The drift chamber has 6 axial layers and 2 stereo layers. It covers 84% of the solid angle and has a momentum resolution of $\sigma_P/P = 0.015 \times \sqrt{1+P^2}$ where P is in GeV/c. The electromagnetic calorimeter is a 24 layer lead sandwich gas proportional sampling shower counter. It covers 94% of the solid angle, has an energy resolution of $\sigma_E/E = .17/\sqrt{E}$ (GeV) and is fully efficient for photons with an energy above .1 GeV. The large acceptance and the high detection efficiency of the Mark III detector enables exclusive reconstruction of high multiplicity J/ψ

decays. Excellent mass resolution is achieved using kinematic constraint fitting on final states with up to 6 photons and 6 charged tracks.

3. Data Analysis

The data sample is obtained from runs taken in 1982, 1983 and 1985. A preliminary analysis based on a smaller data sample has been shown earlier.[10] The present data sample corresponds to 5.8×10^6 produced J/ψ events.

Analysis of $J/\psi \to \gamma\eta\pi^+\pi^-,\ \ \eta \to \gamma\gamma$

The data reduction begins with a selection of events with two oppositely charged tracks and three or more photons. The charged tracks must have hits in both stereo drift chamber layers. No TOF identification is required and all charged tracks are assumed to be π's. The photons are identified as calorimeter showers that are not associated with a charged track. A four-constraint (4C) kinematic fit to the hypothesis $J/\psi \to \gamma\gamma\gamma\ \pi^+\pi^-$ is applied to the two charged tracks and the three highest energy photons. Events with a fit $\chi^2(4C) < 25$ are retained.

A large background comes from the reaction $J/\psi \to \rho\pi$, $\rho \to \pi\pi$. Although these events have two photons, the charged π's can interact in the shower counter and create hadron showers which are falsely identified as photons. This background is reduced by rejecting the event if any pair of the three photons has an invariant mass within .035 GeV/c^2 of the π^0 mass.

If any pair of photons has an invariant mass within .040 GeV/c^2 of the η mass, the event is fit (5C) to the hypothesis $J/\psi \to \gamma\eta\pi^+\pi^-$, $\eta \to \gamma\gamma$. If the fit $\chi^2(5C) > 10$, the event is rejected. If there are multiple fits in a single event the fit with the lowest $\chi^2(5C)$ is used.

The $\eta\pi^+\pi^-$ mass distribution after these cuts is displayed in Fig. 1 (a) and Fig. 1 (b). Observed in this distribution are a large η' signal, a broad structure in the 1-2 GeV/c^2 mass region, and an η_c signal. The efficiency for the decay $J/\psi \to \gamma\eta'$ as determined from Monte Carlo simulation is 26%. The resulting η' branching ratio is

$$B(\psi \to \gamma\eta') = (0.43 \pm .02 \pm .11) \times 10^{-3}.$$

This branching ratio agrees with previous measurements.[11] The fitted η' mass resolution , $\sigma = .005$ GeV/c^2, agrees with Monte Carlo studies. The η_c signal has been previously reported using a smaller data set.[12]

A Dalitz plot for the $\eta\pi\pi$ mass region from 1-2 GeV/c^2 is displayed in Fig. 2 (a). There are clear vertical and horizontal bands from the quasi-two body decay of $J/\psi \to \gamma\ X$, $X \to \delta\pi$, $\delta \to \eta\pi$. The $\eta\pi^\pm$ mass distributions for the 1.2-1.45 GeV/c^2 $\eta\pi\pi$ mass region are shown in Figs. 2(c) and (d). A Breit-Wigner fit to these distributions yields for the δ^+

$$m_{\delta^+} = .986 \pm .003 \text{ GeV/c}^2$$
$$\Gamma_{\delta^+} = .052 \pm .011 \text{ GeV/c}^2$$

and for the δ^-

$$m_{\delta^-} = .989 \pm .004 \text{ GeV/c}^2$$
$$\Gamma_{\delta^-} = .057 \pm .016 \text{ GeV/c}^2$$

which agree with the published values, $m_\delta = .983 \pm .002$ GeV/c^2 and $\Gamma_\delta = .054 \pm .007$ GeV/c^2.[11]

Selecting events with a δ cut, $|m(\eta\pi^\pm) - .983| < 0.05$ GeV/c^2, produces the $\delta\pi$ mass distribution shown in Fig. 3 (a). There is evidence for mass peaks near 1.28 and 1.39 GeV/c^2, and for broad structures between 1.5 and 2.0 GeV/c^2. The converse cut $|m(\eta\pi^\pm) - .983| > 0.1$ GeV/c^2, produces the $\eta\pi\pi$ mass distribution shown in Fig. 3(b). This is featureless except for a rise near 1.8 GeV/c^2 and an η_c signal. The signal near 1.28 GeV/c^2 has a mass and width consistent with those of the $D(1285)$ and the $\eta(1275)$. This signal will be referred to as 'D' in quotes because of its uncertain identity. The signal near 1.39 GeV/c^2 is not identified and will be referred to as X. Neither the $\iota(1440)$ nor the E(1420) appears in either raw mass distribution, but their presence is not ruled out without a partial wave analysis.

The $\eta\pi\pi$ mass regions from 1.1 to 1.54 GeV/c^2 is fit with two non-interfering Breit - Wigner curves and a linear background as shown in Fig. 4 (a). The values for the 'D' mass and width are fixed. The fit yields

$$m_X = 1.382 \pm .006 \text{ GeV/c}^2$$
$$\Gamma_X = .069 \pm .023 \text{ GeV/c}^2.$$

Using a phase space model in a Monte Carlo simulation for the reaction, $\psi \to \gamma\ X$, $X \to \delta\pi$, $\delta \to \eta\pi$, $\eta \to \gamma\gamma$, an efficiency of 40% is obtained. With a total count of 5.8×10^6 produced J/ψ events the resulting product branching ratios are

$$B(\psi \to \gamma\text{'D'}) \times B(\text{'D'} \to \delta^\pm\pi^\mp) \times B(\delta^\pm \to \eta\pi^\pm) = (2.7 \pm 0.8 \pm 0.2) \times 10^{-4}$$
$$B(\psi \to \gamma X) \times B(X \to \delta^\pm\pi^\mp) \times B(\delta^\pm \to \eta\pi^\pm) = (5.2 \pm 1.2 \pm 0.5) \times 10^{-4}.$$

Analysis of $J/\psi \to \gamma\eta\pi^+\pi^-$, $\eta \to \pi^+\pi^-\pi^0$

In this reaction events with 4 charged tracks, whose total charge is zero, and 3 or more photons are selected. A 4-C fit to the hypothesis $J/\psi \to \gamma\gamma\gamma\pi^+\pi^-\pi^+\pi^-$ is applied to the four charged tracks and the three highest energy photons. Events with a χ^2 $(4C)$ > 25 are rejected. If any $\gamma\gamma$ pair mass is within .050 GeV/c^2 of the π^0 mass and if this $\gamma\gamma$ pair plus any $\pi^+\pi^-$ combination has a mass within .050 GeV/c^2 of the η mass, the event is fitted (6C) to the hypothesis $J/\psi \to \gamma\eta\pi^+\pi^-$, $\eta \to \pi^0\pi^+\pi^-$, $\pi^0 \to \gamma\gamma$. If there are multiple fits per event, the fit with the lowest χ^2 is retained. If the χ^2 $(6C)$ > 20 the event is rejected.

The $\eta\pi^+\pi^-$ mass distribution after these cuts is displayed in Figs. 1(c) and (d). The η' and a broad structure in the 1-2 GeV/c^2 mass region are observed. The efficiency from Monte Carlo events is 12% and the resulting η' branching ratio is

$$B(\psi \to \gamma\eta') = (0.33 \pm .02 \pm .07) \times 10^{-3}.$$

This branching ratio agrees with the measurement in the previous section, and the fitted η' mass resolution, $\sigma = .004$ GeV/c^2, agrees with Monte Carlo studies. The statistical evidence for the η_c is not significant.

The $\eta\pi^+\pi^-$ Dalitz plot and the $\eta\pi^+$ and the $\eta\pi^-$ mass distributions for the 1.2-1.45 GeV/c^2 $\eta\pi\pi$ mass region are shown in Figs. 2(b), (e), and (f). There is again a clear $\delta \to \eta\pi$ signal. The mass and width of the δ from a Breit-Wigner fit for the δ^+ are

$$\begin{aligned} m_{\delta^+} &= .987 \pm .003 \text{ GeV/c}^2 \\ \Gamma_{\delta^+} &= .024 \pm .010 \text{ GeV/c}^2 \end{aligned}$$

and for the δ^- are

$$\begin{aligned} m_{\delta^-} &= .978 \pm .004 \text{ GeV/c}^2 \\ \Gamma_{\delta^-} &= .043 \pm .016 \text{ GeV/c}^2 \end{aligned}$$

which are in agreement with the results of the previous section. Applying the δ cut, $|m(\eta\pi^\pm) - .983| < 0.05$ GeV/c^2, yields the $\delta\pi$ mass distribution shown in Fig. 3 (c). The mass distribution obtained with the anti-δ cut, $|m(\eta\pi^\pm) - .983| > 0.1$ GeV/c^2, is shown in Fig. 3 (d). The distributions are similar to those shown in Figs. 3 (a) and (b). Two non-interfering Breit - Wigner curves and a linear background are fit to the δ cut distributions in the mass region from 1.10 to 1.54 GeV/c^2. This is displayed in Fig. 4(b). The values for the 'D' mass and width are fixed and the mean and width of the $X(1390)$ are allowed to vary. The fit yields

$$m_X = 1.400 \pm .007 \text{ GeV}/c^2$$
$$\Gamma_X = .062 \pm .016 \text{ GeV}/c^2$$

A Monte Carlo efficiency of 15% is obtained using a phase space model for the reaction, $\psi \to \gamma X$, $X \to \delta\pi$, $\delta \to \eta\pi$, $\eta \to \pi^0\pi^+\pi^-$. The resulting product branching ratios are,

$$B(\psi \to \gamma\text{'D'}) \times B(\text{'D'} \to \delta^{\pm}\pi^{\mp}) \times B(\delta^{\pm} \to \eta\pi^{\pm}) = (3.2 \pm 1.1 \pm 0.3) \times 10^{-4}$$
$$B(\psi \to \gamma X) \times B(X \to \delta^{\pm}\pi^{\mp}) \times B(\delta^{\pm} \to \eta\pi^{\pm}) = (5.2 \pm 1.8 \pm 0.5) \times 10^{-4}.$$

4. Discussion of Results

The quasi-two body decay, $J/\psi \to \gamma\delta\pi$, $\delta \to \eta\pi$, is clearly observed. In this mode, two signals, the 'D' and the $X(1390)$, appear in the two η decay modes. The higher mass region, 1.5-2.0 GeV/c^2, does not have sufficient events in both modes to clearly observe consistent structures.

The 'D' signal has a mass consistent with the $D(1285)$ and the $\eta(1275)$. If this signal is the $D(1285)$, the observed branching ratio is not in contradiction with the published upper limit of 0.6%.[2]

The $X(1390)$ signal may have been seen before in a bubble chamber experiment studying $p\bar{p} \to 3\pi^+3\pi^-\pi^0$ reactions.[13] An $\eta\pi\pi$ signal was observed at 1.390 GeV/c^2 and this was suggested to be the E(1420) shifted to a lower mass because of the rapid decrease of phase space. In this analysis there is no clear indication for the $\iota(1440)$ or the E(1420) in raw mass distributions. There is a pronounced dip at 1.440 GeV/c^2 above the peak at 1.390 GeV/c^2. Strong interference between the $\iota(1440)$ or the E(1420) and the other resonances in this mass region could possibly produce such a shape. This can neither be proven nor ruled out without a partial wave analysis.

The shape of the $\eta\pi\pi$ mass distribution is quite different from the $K\bar{K}\pi$ mass distribution observed in $J/\psi \to \gamma K\bar{K}\pi$.[14] In the $K\bar{K}\pi$ mass spectrum the $\iota(1440)$ peaks near 1.440 GeV/c^2 and has a full width of $\sim$ .100 GeV/c^2. In contrast, the $\eta\pi\pi$ mass distribution has a peak near 1.390 GeV/c^2 and a dip or a cusp near KK^* threshold where the $\iota(1440)$ in the $K\bar{K}\pi$ mode reaches its peak mass value. A spin-parity study of the $\eta\pi\pi$ system may clarify this situation.

We gratefully acknowledge the dedicated efforts of the SPEAR and LINAC operations groups at SLAC. Also we would like to thank the technical and engineering staffs of Group D at SLAC and the collaborating universities. One of us (G.E.) wishes to thank the Alexander von Humboldt Foundation for support. This work was supported in part by the U.S. National Science Foundation and the U.S. Department of Energy under Contracts No. DE-AC03-76SF00515, No. DE-AC02-76ER01195, No. DE-AC03-81ER40050, and No. DE-AM03-76SF00034.

FIGURE CAPTIONS

1. The $\eta\pi^+\pi^-$ mass distribution in the mass regions (a) .0-3.1 GeV/c^2 and (b) 1.0-3.1 GeV/c^2 from the mode, $J/\psi \to \gamma\eta\pi^+\pi^-$, $\eta \to \gamma\gamma$. The $\eta\pi^+\pi^-$ mass distribution in the mass regions (c) .0-3.1 GeV/c^2 and (d) 1.0-3.1 GeV/c^2 from the mode, $J/\psi \to \gamma\eta\pi^+\pi^-$, $\eta \to \pi^+\pi^-\pi^0$.
2. The $\eta\pi\pi$ Dalitz plot (a), for the $\eta\pi\pi$ mass region from 1 to 2 GeV/c^2, from the $J/\psi \to \gamma\eta\pi^+\pi^-$, $\eta \to \gamma\gamma$ mode. The $\eta\pi\pi$ Dalitz plot (b), for the $\eta\pi\pi$ mass region from 1 to 2 GeV/c^2, from the $J/\psi \to \gamma\eta\pi^+\pi^-$, $\eta \to \pi^+\pi^-\pi^0$ mode. The $\eta\pi^+$ mass distribution (c) and $\eta\pi^-$ mass distribution (d), with Breit-Wigner fits for the $\eta\pi\pi$ mass region from 1.2 to 1.45 GeV/c^2, from th e $J/\psi \to \gamma\eta\pi^+\pi^-$, $\eta \to \gamma\gamma$ mode. The $\eta\pi^+$ mass distribution (e), and $\eta\pi^-$ mass distribution (f) for the $\eta\pi\pi$ mass region from 1.2 to 1.45 GeV/c^2, with Breit-Wigner fits from the $J/\psi \to \gamma\eta\pi^+\pi^-$, $\eta \to \pi^+\pi^-\pi^0$ mode.
3. The $\eta\pi\pi$ mass distribution (a) with the 'δ' cut and the $\eta\pi\pi$ mass distribution (b) with the 'anti-δ' cut from the $J/\psi \to \gamma\eta\pi^+\pi^-$, $\eta \to \gamma\gamma$ mode. The $\eta\pi\pi$ mass distribution (c) with the 'δ' cut and the $\eta\pi\pi$ mass distribution (d) with the 'anti-δ' cut from the $J/\psi \to \gamma\eta\pi^+\pi^-$, $\eta \to \pi^+\pi^-\pi^0$ mode.
4. The $\eta\pi\pi$ mass distribution (a) with the 'δ' cut and a Breit-Wigner fit from the $J/\psi \to \gamma\eta\pi^+\pi^-$, $\eta \to \gamma\gamma$ mode. The $\eta\pi\pi$ mass distribution (b) with the 'δ' cut and a Breit-Wigner fit f rom the $J/\psi \to \gamma\eta\pi^+\pi^-$, $\eta \to \pi^+\pi^-\pi^0$ mode.

1. C. Edwards *et al.*, *Phys. Rev. Lett.* **48**, 458 (1982)
2. D. Scharre *et al.*, *Phys. Lett.* **97B**, 321 (1980)
3. The ι was observed to decay to $\delta\pi$ and has J^{PC}=0^{-+}. C. Edwards *et al.*, *Phys. Rev. Lett.* **49**, 259 (1982)
   The $E(1420)$ was observed to largely decay to $\delta\pi$ and J^{PC}=O^{-+}. P. Baillon *et al.*, *Nuovo Cimento* **50A**, 393(1967)
   S. Chung *et al.*, *Phys. Rev. Lett.* **55**, 779 (1985)
   The $E(1420)$ was observed to largely decay to KK^* and J^{PC}=1^{++}. C. Dionisi *et al.*, *Nucl. Phys.* **B169**, 1 (1980)
   T. Armstrong *et al.*, *Phys. Lett.* **146B**, 273 (1984)
4. R. Cahn and P. Landshoff, *Nucl. Phys.* **B266**, 451(1986)
5. C. Defoix *et al.*, *Nucl. Phys.* **B44**, 125 (1986)
   A. Ando *et al.*, KEK Preprint 86-3, submitted to Phys. Rev. Letts.
   O. Villalobos Baillie, Proceedings of the International Europhysics Conference on High Energy Physics (Bari,1985), p. 314.
   T. Mouthuy, Proceedings of the International Europhysics Conference on High Energy Physics (Bari,1985),p. 320.
6. P. Baillon *et al.*, *Nuovo Cimento* **50A**, 393(1967)
   C. Dionisi *et al.*, *Nucl. Phys.* **B169**, 1 (1980)
7. D. Scharre *et al.*, *Phys. Lett.* **97B**, 321 (1980)
8. M. Stanton *et al.*, *Phys. Rev. Lett.* **42**, 346 (1979)
   A. Ando *et al.*, KEK Preprint 84-7, submitted to the XXII International Conference on High Energy Physics, Leipzig, 19-25 July, 1984.
9. D. Bernstein *et al.*, *Nucl. Inst. Meth.* **226**, 301 (1984)
   J. Roehrig *et al.*, *Nucl. Inst. Meth.* **226**, 319 (1984)
   W. Toki *et al.*, *Nucl. Inst. Meth.* **219**, 479 (1984)
10. W. Toki, invited talk, Topical Conference, SLAC Summer Institute on Particle Physics, 1983
11. C. Wolh *et al.*, *Rev. Mod. Phys.* **56**, S1 (1984)
12. R. Baltrusaitus *et al.*, *Phys. Rev.* **D33**, 629 (1986)
13. C. Defoix *et al.*, *Nucl. Phys.* **B44**, 125 (1986)
14. J. Richman, Ph.d. Thesis, California Instutite of Technology, CALT-68-1231

FIGURE 1

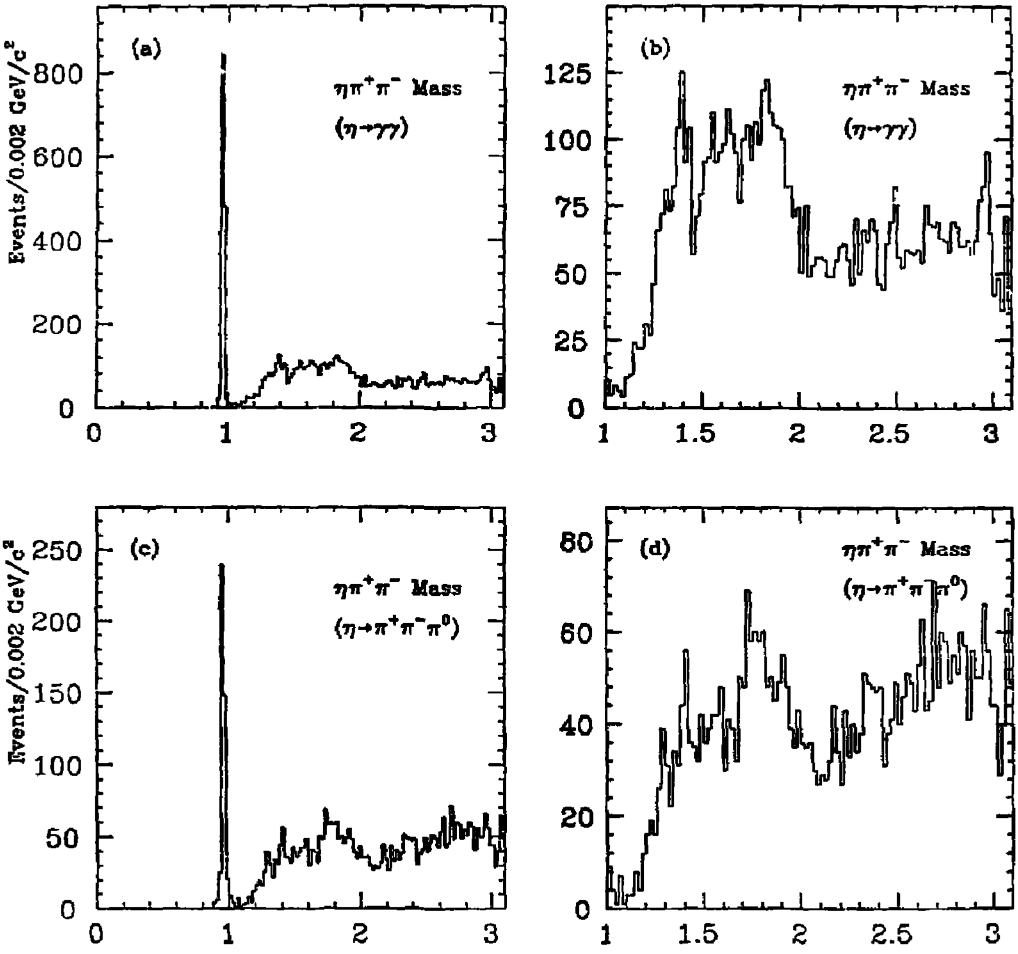

(a)
$\eta\pi^+\pi^-$ Mass
$(\eta\to\gamma\gamma)$
(b)
$\eta\pi^+\pi^-$ Mass
$(\eta\to\gamma\gamma)$
(c)
$\eta\pi^+\pi^-$ Mass
$(\eta\to\pi^+\pi^-\pi^0)$
(d)
$\eta\pi^+\pi^-$ Mass
$(\eta\to\pi^+\pi^-\pi^0)$
Events/0.002 GeV/c^2
0
200
400
600
800
0
25
50
75
100
125
0
50
100
150
200
250
0
20
40
60
80
0
1
2
3
1
1.5
2
2.5
3

FIGURE 2

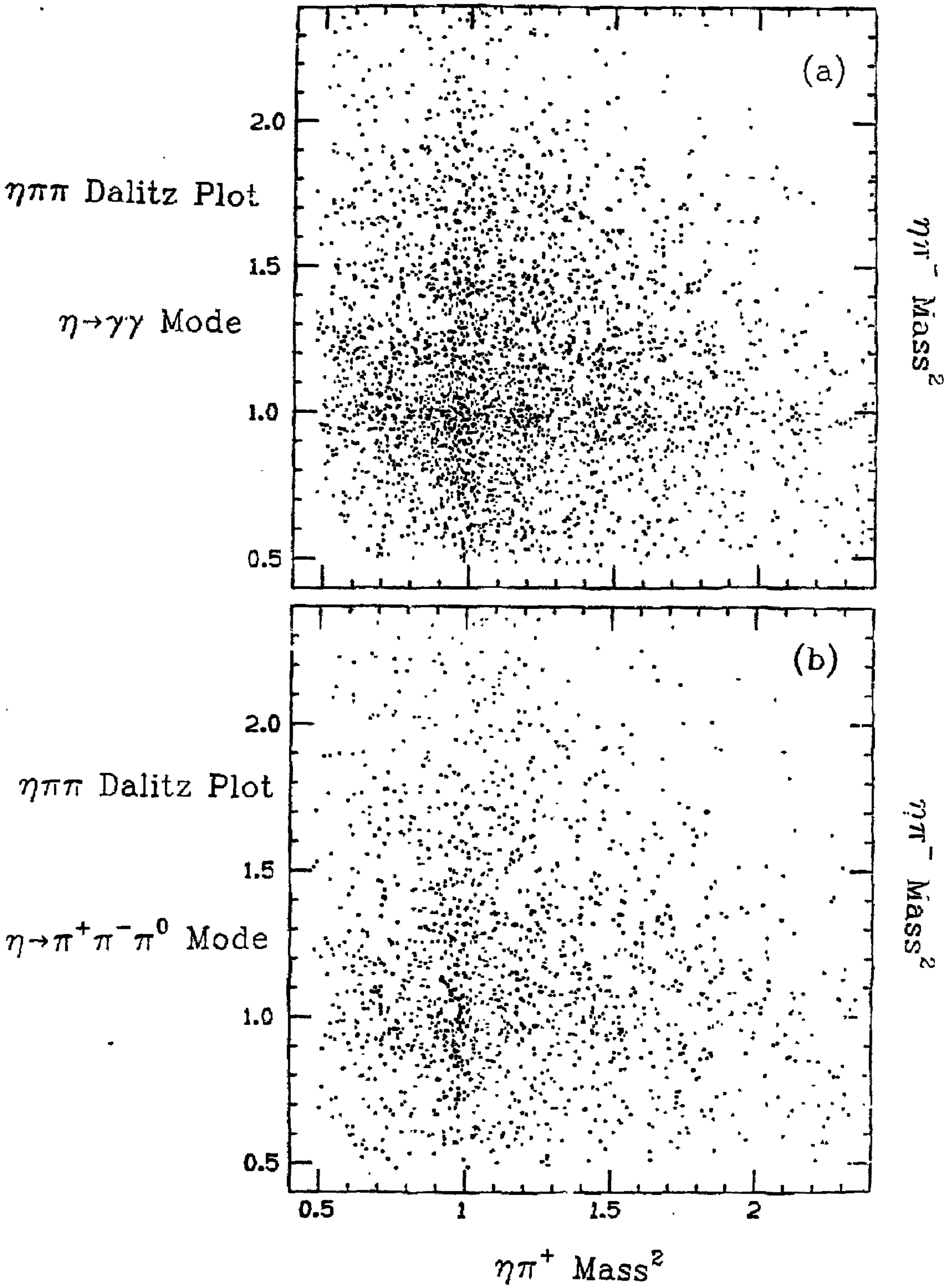
(a)
ηππ Dalitz Plot
η→γγ Mode
ηπ⁻ Mass²
2.0
1.5
1.0
0.5
(b)
ηππ Dalitz Plot
η→π⁺π⁻π⁰ Mode
ηπ⁻ Mass²
2.0
1.5
1.0
0.5
0.5
1
1.5
2
ηπ⁺ Mass²

FIGURE 2

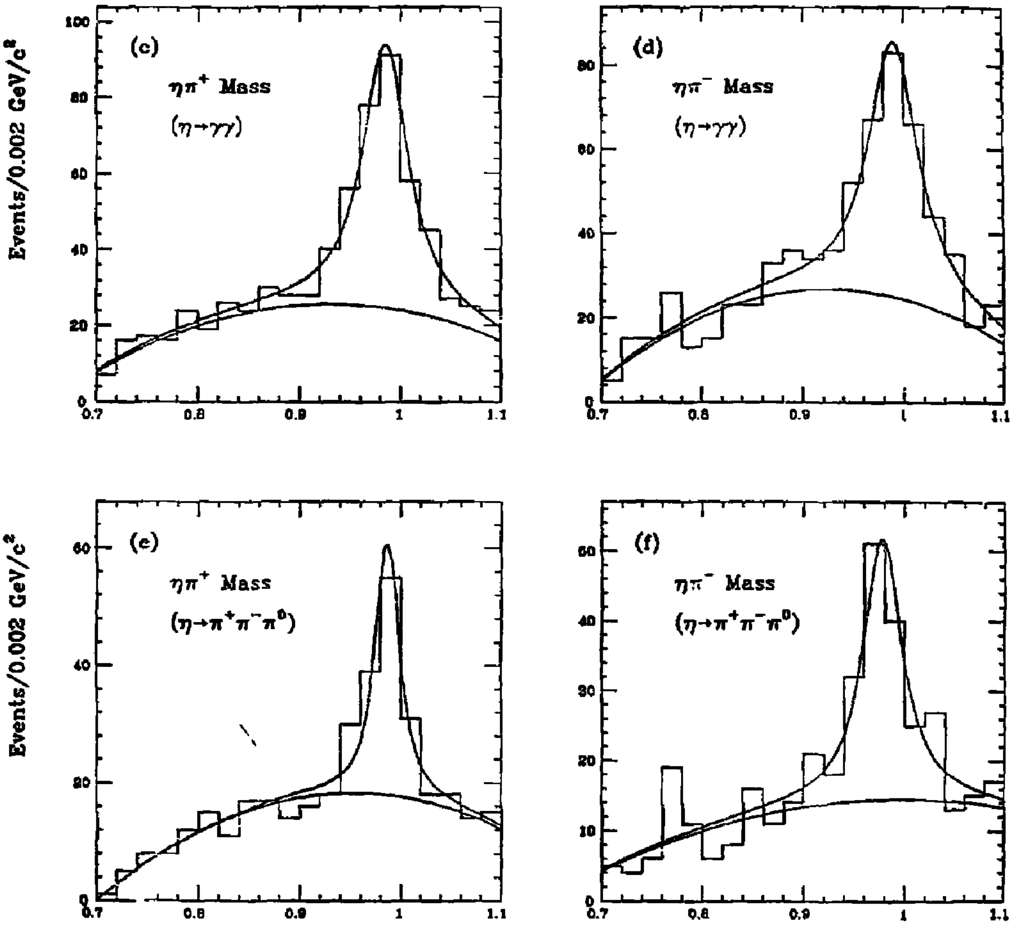

Events/0.002 GeV/c²
(c)
ηπ⁺ Mass
(η→γγ)
(d)
ηπ⁻ Mass
(η→γγ)
Events/0.002 GeV/c²
(e)
ηπ⁺ Mass
(η→π⁺π⁻π⁰)
(f)
ηπ⁻ Mass
(η→π⁺π⁻π⁰)

FIGURE 3

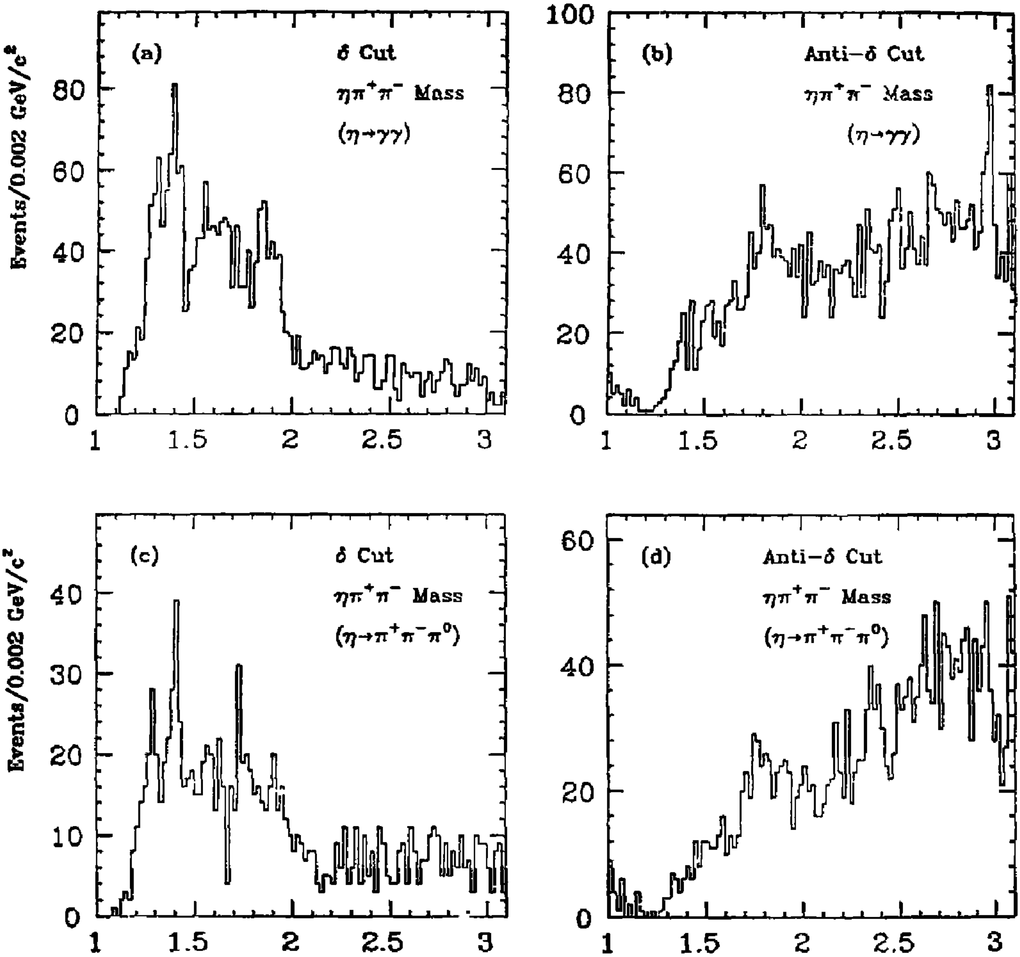

(a)
δ Cut
ηπ⁺π⁻ Mass
(η→γγ)
(b)
Anti–δ Cut
ηπ⁺π⁻ Mass
(η→γγ)
(c)
δ Cut
ηπ⁺π⁻ Mass
(η→π⁺π⁻π⁰)
(d)
Anti–δ Cut
ηπ⁺π⁻ Mass
(η→π⁺π⁻π⁰)
Events/0.002 GeV/c²
0
20
40
60
80
100
10
30
1
1.5
2
2.5
3

FIGURE 4

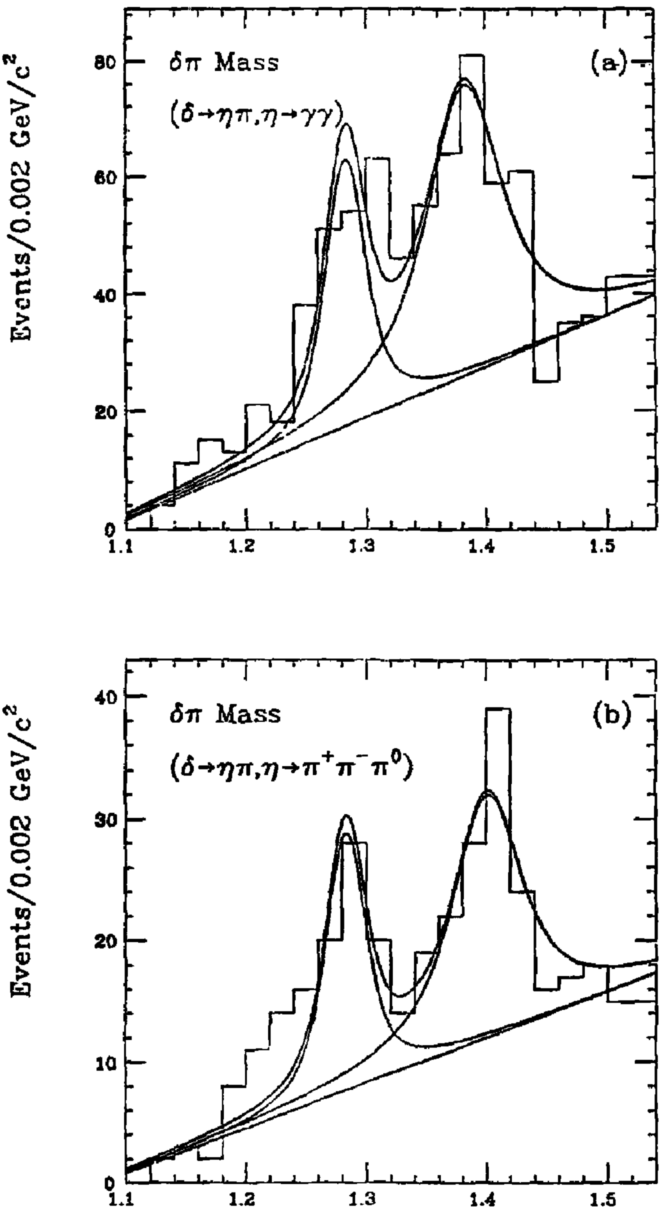

δπ Mass
(δ→ηπ,η→γγ)
(a)
Events/0.002 GeV/c²
0
20
40
60
80
1.1
1.2
1.3
1.4
1.5
δπ Mass
(δ→ηπ,η→π⁺π⁻π⁰)
(b)
Events/0.002 GeV/c²
0
10
20
30
40
1.1
1.2
1.3
1.4
1.5